

Two dimensional electron gases in polycrystalline MgZnO/ZnO heterostructures grown by rf-sputtering process

Huai-An Chin,¹ I-Chun Cheng,^{1,a)} Chih-I Huang,¹ Yuh-Renn Wu,¹ Wen-Sen Lu,² Wei-Li Lee,² Jian Z. Chen,^{3,b)} Kuo-Chuang Chiu,⁴ and Tzer-Shen Lin⁴

¹Department of Electrical Engineering and Graduate Institute of Photonics and Optoelectronics, National Taiwan University, Taipei 10617, Taiwan

²Institute of Physics, Academia Sinica, Taipei 11529, Taiwan

³Institute of Applied Mechanics, National Taiwan University, Taipei 10617, Taiwan

⁴Material and Chemical Research Laboratories, Industrial Technology Research Institute, Hsinchu 31040, Taiwan

(Received 26 May 2010; accepted 4 July 2010; published online 7 September 2010)

This paper reports the formation of two-dimensional electron gas (2DEG) in rf-sputtered defective polycrystalline MgZnO/ZnO heterostructure via the screening of grain boundary potential by polarization-induced charges. As the MgZnO thickness increases, the sheet resistance reduces rapidly and then saturates. The enhancement of the interfacial polarization effect becomes stronger, corresponding to a larger amount of resistance reduction, when the Mg content in the cap layer increases. Monte Carlo method by including grain boundary scattering effect as well as 2D finite-element-method Poisson and drift-diffusion solver is applied to analyze the polycrystalline heterostructure. The experimental and Monte Carlo simulation results show good agreement. From low temperature Hall measurement, the carrier density and mobility are both independent of temperature, indicating the formation of 2DEG with roughness scattering at the MgZnO/ZnO interface. © 2010 American Institute of Physics. [doi:10.1063/1.3475500]

I. INTRODUCTION

ZnO has shown great potential in optoelectronic device applications, such as UV light emitters, high-power electronic devices, and transparent electronics.^{1–13} Like GaN, with which the high electron mobility transistor (HEMT) heterostructure (AlGaIn/GaN) has been realized by the formation of two-dimensional electron gas (2DEG) via electric polarization effects, the polarization difference between two heterojunction materials.¹⁴ ZnO also exhibits similar effect in MgZnO/ZnO heterostructure but with several advantages over AlGaIn/GaN, including a higher saturation velocity, a lower lattice mismatch, and the capability for bulk growth.^{15–18}

ZnO can be alloyed with MgO to form $Mg_xZn_{1-x}O$, in which the bandgap is dependent on the Mg content x .¹⁹ In this fashion, the degree of polarization in MgZnO/ZnO heterostructure can be adjusted. Several studies in regard to the 2DEG formation at MgZnO/ZnO single-crystalline system have been reported.^{20–22} Attributing to the polarization effect, large amount of sheet carrier concentration is induced and thus the electrical conductance of the high quality single-crystalline or polycrystalline system is greatly enhanced. However, these are mostly demonstrated by pulse laser deposition or molecular beam epitaxy (MBE), which is not suitable for low-cost large-area electronic applications. Therefore, in this paper, we investigate 2DEG formation in a much defective *rf-sputtered* polycrystalline MgZnO/ZnO material system. One key point for this study is to find out whether the 2DEG can be observed under the influence of the grain

boundaries and/or other structural defects. Our previous simulation work by Monte Carlo method²³ indicates that the grain boundary potential of a polycrystalline MgZnO/ZnO heterostructure can be screened by the induced carriers. Thus the 2DEG induced by the polarization and piezoelectric effects can occur in a defective polycrystalline MgZnO/ZnO material system. Here, we report the experimental evidence. The result can be further applied to the design and fabrication of low-cost large-area heterojunction thin film transistors.

II. EXPERIMENT

First a 300-nm-thick ZnO thin film is rf-sputtered on Corning Eagle-2000 glass at room temperature, followed by a post-annealing at 600 °C for 30 min to reinforce the grain formation.^{24,25} Then 200-nm-thick titanium is deposited by e-beam evaporation and patterned as the coplanar electrical contacts.^{26,27} Finally, $Mg_xZn_{1-x}O$ layer with various thicknesses and Mg contents ($x=0.15, 0.2, 0.3, 0.4,$ and 0.5) is rf-sputtered at room temperature upon ZnO to form the heterostructure. The deposition conditions for the ZnO and MgZnO layers are: argon/oxygen flow rate ratio of 6/1, power density of 2.2 W/cm², and processing pressure of 10 mtorr. The crystalline structure and the grain size of the ZnO layer are investigated by x-ray diffraction (XRD). The electrical characteristics of the heterostructure are evaluated by both coplanar two-point current-voltage measurement and Hall measurement with van der Pauw geometry.

^{a)}Electronic mail: ichuncheng@cc.ee.ntu.edu.tw.

^{b)}Electronic mail: jchen@ntu.edu.tw.

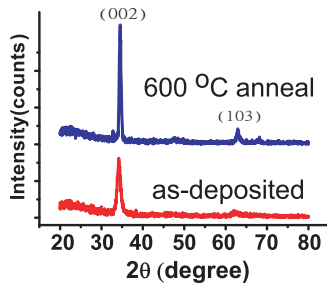


FIG. 1. (Color online) XRD pattern of rf-sputtered ZnO layer before and after 600 °C post-deposition annealing.

III. RESULTS AND DISCUSSION

Figure 1 shows the XRD patterns of ZnO thin films before and after 600 °C annealing, which indicates the polycrystalline nature of the ZnO layers with (002) preferred orientation. Despite that the as-deposited ZnO already reveals certain crystallinity, the post-annealing process reinforces the grain formation and improves the quality of ZnO. This post-annealing process turns out to be a critical step in observing 2DEG in our polycrystalline MgZnO/ZnO heterostructure. Without this step, no improvement of electrical conductance is obtained, which is attributed to small grain sizes with large amount of grain boundary defects in the as-deposited material system.

Figure 2 shows the sheet resistance of the $\text{Mg}_x\text{Zn}_{1-x}\text{O}/\text{ZnO}$ heterostructure versus $\text{Mg}_x\text{Zn}_{1-x}\text{O}$ thickness for $x=0.15, 0.2, 0.3, 0.4,$ and 0.5 . The initial sheet resistance of the 600 °C annealed ZnO layer is $\sim 10^6 \Omega$. After depositing $\text{Mg}_x\text{Zn}_{1-x}\text{O}$ cap layer, the electrical resistance of the heterostructure reduces by two to three orders of magnitude. The amount of reduction increases rapidly and then saturates as the $\text{Mg}_x\text{Zn}_{1-x}\text{O}$ thickness increases. The onset thickness of the saturation depends on the Mg content x in $\text{Mg}_x\text{Zn}_{1-x}\text{O}$. As the Mg content increases, the degree of polarization effect is enhanced, which introduces larger amount of carriers at the interface and thus provides stronger screening effect on the grain boundary potential. Therefore, a greater amount of resistance reduction and a smaller onset thickness are observed in the case of larger Mg content.

In polycrystalline system, the electron transport property is greatly influenced by the grain boundary potential.²⁸ The 2DEG, formed at the interface between MgZnO and ZnO,

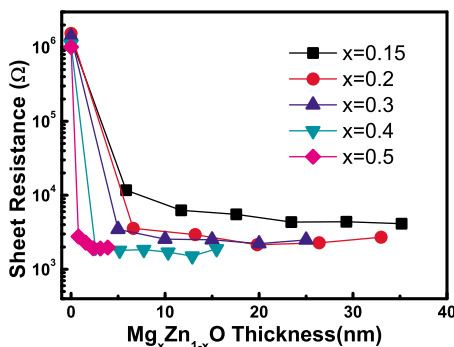


FIG. 2. (Color online) Sheet resistance of polycrystalline $\text{Mg}_x\text{Zn}_{1-x}\text{O}/\text{ZnO}$ heterostructure vs thickness of $\text{Mg}_x\text{Zn}_{1-x}\text{O}$ cap layer for $x=0.15, 0.2, 0.3, 0.4,$ and 0.5 . The lines are guides to the eyes.

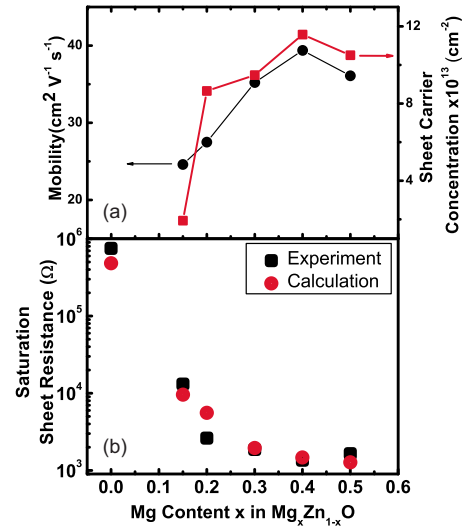


FIG. 3. (Color online) (a) Hall mobility and sheet carrier concentration of $\text{Mg}_x\text{Zn}_{1-x}\text{O}/\text{ZnO}$ heterostructure in saturation as functions of Mg content x . (b) Comparison of experimental and calculated saturation sheet resistances as functions of Mg content x . The lines are guides to the eye.

reduces the grain boundary potential, thereby improving the mobility.²³ The Hall mobility and sheet carrier concentration in our annealed polycrystalline ZnO thin film are $1.46 \text{ cm}^2\text{V}^{-1}\text{s}^{-1}$ and $5.69 \times 10^{12} \text{ cm}^{-2}$, respectively. As shown in Fig. 3(a), both the mobility and the sheet carrier concentration of the MgZnO/ZnO heterostructure in saturation show positive correlations with the Mg content and reach maximum values of $39.4 \text{ cm}^2\text{V}^{-1}\text{s}^{-1}$ and $1.15 \times 10^{14} \text{ cm}^{-2}$ at $x=0.4$. The carrier concentrations are measured using two different experimental setups in two different laboratories. The same order of magnitude is acquired. The high carrier concentration, one order of magnitude larger than that measured with samples grown by radical source MBE,²⁰ is probably due to the high defect density in our samples, contributing more carriers to the interface.

We further study the polycrystalline heterostructure by using Monte Carlo method with the effects of grain boundary barrier impurity scattering as well as phonon scattering included.²⁹ Then the 2D finite-element-method Poisson and drift-diffusion solver is used to determine the strength of the grain boundary potential, carrier density, and the effects of polarization and carrier screening in the device.²³ Figure 3(b) shows the comparison between experimental and simulated saturation sheet resistance as functions of Mg content x . The simulation result, performed with a grain size of 75 nm, grain boundary trap level of 0.85 eV, grain boundary trap density of $5 \times 10^{12} \text{ cm}^{-2}$, and background bulk doping density of $1 \times 10^{18} \text{ cm}^{-3}$, agrees well with our experimental result. The decrease in conductance enhancement at $x=0.5$ observed in experiment may be caused by the phase separation of $\text{Mg}_x\text{Zn}_{1-x}\text{O}$ at large x (Refs. 21 and 30) due to the two end components of MgZnO alloy system, ZnO and MgO, crystallize in different structures, wurtzite and rocksalt, respectively. In comparison to the single crystalline system, Tampo *et al.*²⁰ discover that the mobility increases first and saturates at x of ~ 0.2 as the Mg content x increases in $\text{Mg}_x\text{Zn}_{1-x}\text{O}/\text{ZnO}$ heterostructure, yet the sheet carrier con-

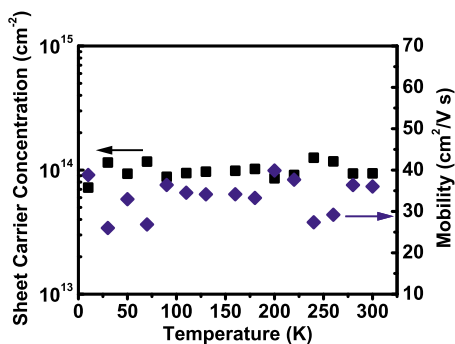


FIG. 4. (Color online) Hall mobility and carrier concentration of $\text{Mg}_{0.3}\text{Zn}_{0.7}\text{O}/\text{ZnO}$ heterostructure with $\text{Mg}_{0.3}\text{Zn}_{0.7}\text{O}$ capping layer thickness of ~ 30 nm as functions of temperature.

centration remains constant throughout the Mg concentration up to $x=0.45$. They further report that both the mobility and sheet carrier concentration increase as the Mg content x increases up to 0.6, when the defect-induced phase separation is suppressed in $\text{Mg}_x\text{Zn}_{1-x}\text{O}/\text{ZnO}$ heterostructure by a thick ZnO buffer layer.²¹ Our experimental result implies a competition between the grain boundary screening by the polarization-induced charges and the defect-induced phase separation at high Mg content.

To validate the charges are indeed two-dimensional and are induced by the polarization effect at the interface, we perform low temperature Hall measurement to obtain carrier density and mobility as a function of temperature, as shown in Fig. 4. No significant variation is found as the temperature changes, indicating that the dominant carriers are not resulting from the thermal activation. In addition, the measured sheet carrier density is about 10^{14} cm^{-2} , which is much higher than those in the pure ZnO or MgZnO layers. This supports that the reduction in resistivity is due to the formation of 2DEG at the MgZnO/ZnO interface. Theoretically, the mobility of a high quality crystalline semiconductor increases as the temperature decreases due to the reduction in phonon scattering; the mobility of a defective semiconductor should decrease as the temperature decreases due to ionized impurity scattering.³¹ Our sample shows a temperature independent trend on carrier mobility, which is related to surface roughness scattering of 2DEG at MgZnO/ZnO interface.³² The improvement of the surface smoothness would be essential to achieve higher mobility.

IV. SUMMARY

We study the formation of 2DEG in rf-sputtered polycrystalline MgZnO/ZnO heterostructure via the screening of grain boundary potential by polarization-induced charges. The sheet resistance reduces rapidly and then saturates as the MgZnO thickness increases. Both the mobility and the sheet carrier concentration in saturation increase as the Mg content is raised and reach maxima of 39.4 $\text{cm}^2\text{V}^{-1}\text{s}^{-1}$ and 1.15×10^{14} cm^{-2} at $x=0.4$ at room temperature. The experimental and simulated saturation sheet resistance show good agreement. Both carrier concentration and mobility are temperature independent, indicating the formation of 2DEG with roughness scattering at the MgZnO/ZnO interface. Our result

suggests that polycrystalline MgZnO/ZnO material system can be a potential candidate for the application of low-cost large-area HEMT devices.

ACKNOWLEDGMENTS

The authors would like to thank Material and Chemical Research Laboratories, Industrial Technology Research Institute for the financial and technical support. I.C.C. and J.Z.C. gratefully acknowledge the funding support from the National Science Council of Taiwan, under Grant Nos. NSC 98-2221-E-002-186 and NSC 98-2120-M-002-005 (I.C.C.); NSC 98-2221-E-002-169 and NSC 98-2627-M-002-015 (J.Z.C.).

- ¹D. C. Look, *Mater. Sci. Eng.*, **B 80**, 383 (2001).
- ²C. R. Gorla, N. W. Emanetoglu, S. Liang, W. E. Mayo, Y. Lu, M. Wraback, and H. Shen, *J. Appl. Phys.* **85**, 2595 (1999).
- ³S. O. Kucheyev, J. E. Bradley, J. S. Williams, C. Jagadish, and M. V. Swain, *Appl. Phys. Lett.* **80**, 956 (2002).
- ⁴W. B. Jackson, in *Flexible Electronics: Materials and Applications*, edited by W. S. Wong and A. Salleo (Springer, New York, 2009), p. 107.
- ⁵H.-H. Shieh, I.-C. Cheng, J. Z. Chen, C.-C. Hsiao, P.-C. Lin, and Y.-H. Yeh, *J. Electrochem. Soc.* **157**, H750 (2010).
- ⁶E. Fortunato, P. Barquinha, A. Pimentel, A. Gonçalves, A. Marques, L. Pereira, and R. Martins, *Thin Solid Films* **487**, 205 (2005).
- ⁷Dhananjay and S. B. Krupanidhi, *J. Appl. Phys.* **101**, 123717 (2007).
- ⁸P. F. Carcia, R. S. Mclean, M. H. Reilly, M. K. Crawford, E. N. Blanchard, A. Z. Kattamis, and S. Wagner, *J. Appl. Phys.* **102**, 074512 (2007).
- ⁹E. Fortunato, L. Pereira, P. Barquinha, I. Ferreira, R. Prabaharan, G. Gonçalves, A. Gonçalves, and R. Martins, *Philos. Mag.* **89**, 2741 (2009).
- ¹⁰R. L. Hoffman, *J. Appl. Phys.* **95**, 5813 (2004).
- ¹¹Y. Ye, R. Lim, and J. M. White, *J. Appl. Phys.* **106**, 074512 (2009).
- ¹²R. L. Hoffman, B. J. Norris, and J. F. Wager, *Appl. Phys. Lett.* **82**, 733 (2003).
- ¹³R. Martins, E. Fortunato, P. Nunes, I. Ferreira, and A. Marques, *J. Appl. Phys.* **96**, 1398 (2004).
- ¹⁴O. Ambacher, J. Smart, J. R. Shealy, N. G. Weimann, K. Chu, M. Murphy, W. J. Schaff, L. F. Eastman, R. Dimitrov, L. Wittmer, M. Stutzmann, W. Rieger, and J. Hilsenbeck, *J. Appl. Phys.* **85**, 3222 (1999).
- ¹⁵J. D. Albrecht, P. P. Ruden, S. Limpijumnong, W. R. L. Lambrecht, and K. F. Brennan, *J. Appl. Phys.* **86**, 6864 (1999).
- ¹⁶A. Ohtomo, M. Kawasaki, T. Koida, K. Masubuchi, H. Koinuma, Y. Sakurai, Y. Yoshida, T. Yasuda, and Y. Segawa, *Appl. Phys. Lett.* **72**, 2466 (1998).
- ¹⁷A. Ohtomo, M. Kawasaki, I. Ohkubo, H. Koinuma, T. Yasuda, and Y. Segawa, *Appl. Phys. Lett.* **75**, 980 (1999).
- ¹⁸A. N. Westmeyer, S. Mahajan, K. K. Bajaj, J. Y. Lin, H. X. Jiang, D. D. Koleske, and R. T. Senger, *J. Appl. Phys.* **99**, 013705 (2006).
- ¹⁹T. Minemoto, T. Negami, S. Nishiwaki, H. Takakura, and Y. Hamakawa, *Thin Solid Films* **372**, 173 (2000).
- ²⁰H. Tampo, H. Shibata, K. Matsubara, A. Yamada, P. Fons, S. Niki, M. Yamagata, and H. Kanie, *Appl. Phys. Lett.* **89**, 132113 (2006).
- ²¹H. Tampo, H. Shibata, K. Maejima, A. Yamada, K. Matsubara, P. Fons, S. Kashiwaya, S. Niki, Y. Chiba, T. Wakamatsu, and H. Kanie, *Appl. Phys. Lett.* **93**, 202104 (2008).
- ²²M. Yano, K. Hashimoto, K. Fujimoto, K. Koike, S. Sasa, M. Inoue, Y. Uetsuji, T. Ohnishi, and K. Inaba, *J. Cryst. Growth* **301–302**, 353 (2007).
- ²³C.-I. Huang, H.-A. Chin, Y.-R. Wu, I.-C. Cheng, J. Z. Chen, K.-C. Chiu, and T.-S. Lin, *IEEE Trans. Electron Devices* **57**, 696 (2010).
- ²⁴T. Hiramatsu, M. Furuta, H. Furuta, T. Matsuda, C. Li, and T. Hiro, *J. Cryst. Growth* **311**, 282 (2009).
- ²⁵P. Nunes, E. Fortunato, and R. Martins, *Thin Solid Films* **383**, 277 (2001).
- ²⁶S. Kim, B. S. Kang, F. Ren, Y. W. Heo, K. Ip, D. P. Norton, and S. J. Pearton, *Appl. Phys. Lett.* **84**, 1904 (2004).
- ²⁷Y. Shimura, K. Nomura, H. Yanagi, T. Kamiya, M. Hirano, and H. Hosono, *Thin Solid Films* **516**, 5899 (2008).
- ²⁸F. M. Hossain, J. Nishii, S. Takagi, A. Ohtomo, T. Fukumura, H. Fujioka,

- H. Ohno, H. Koinuma, and M. Kawasaki, *J. Appl. Phys.* **94**, 7768 (2003).
- ²⁹Y.-R. Wu, M. Singh, and J. Singh, *IEEE Trans. Electron Devices* **53**, 588 (2006).
- ³⁰A. Malashevich and D. Vanderbilt, *Phys. Rev. B* **75**, 045106 (2007).
- ³¹J. Singh, *Physics of Semiconductors and their Heterostructures* (McGraw-Hill, New York, 1993).
- ³²R. Gottinger, A. Gold, G. Abstreiter, G. Weimann, and W. Schlapp, *Europhys. Lett.* **6**, 183 (1988).